Cancer Immunology, Immunotherapy (2020) 69:1905–1916
https://doi.org/10.1007/s00262-020-02594-9

ORIGINAL ARTICLE

Prognostic role of PD-L1 and immune-related gene expression profiles in giant cell tumors of bone

Jasna Metovic[1] · Laura Annaratone[2,3] · Alessandra Linari[1] · Simona Osella-Abate[2] · Chiara Musuraca[1] · Francesca Veneziano[1] · Chiara Vignale[1] · Luca Bertero[2] · Paola Cassoni[2] · Nicola Ratto[4] · Alessandro Comandone[5,6] · Giovanni Grignani[7] · Raimondo Piana[4] · Mauro Papotti[1,8]

Received: 19 August 2019 / Accepted: 27 April 2020 / Published online: 6 May 2020

Abstract

Giant cell tumor of bone (GCTB) is a locally aggressive and rarely metastatic tumor, with a relatively unpredictable clinical course. A retrospective series of 46 GCTB and a control group of 24 aneurysmal bone cysts (ABC) were selected with the aim of investigating the PD-L1 expression levels and immune-related gene expression profile, in correlation with clinicopathological features. PD-L1 and Ki67 were immunohistochemically tested in each case. Furthermore, comprehensive molecular analyses were carried out using NanoString technology and nCounter PanCancer Immune Profiling Panel, and the gene expression results were correlated with clinicopathological characteristics. PD-L1 expression was observed in 13/46 (28.3%) GCTB (and in 1/24, 4.2%, control ABC, only) and associated with a shorter disease free interval according to univariate analysis. Moreover, in PD-L1-positive lesions, three genes (*CD27*, *CD6* and *IL10)* were significantly upregulated ($p < 0.01$), while two were downregulated (*LCK* and *TLR8*, showing borderline significance, $p = 0.06$). Interestingly, these genes can be related to maturation and immune tolerance of bone tissue microenvironment, suggesting a more immature/anergic phenotype of giant cell tumors. Our findings suggest that PD-L1 immunoreactivity may help to select GCTB patients with a higher risk of recurrence who could potentially benefit from immune checkpoint blockade.

Keywords Giant cell tumor of bone · PD-L1 · Immune-related genes · NanoString technology · Prognosis

Electronic supplementary material The online version of this article (https://doi.org/10.1007/s00262-020-02594-9) contains supplementary material, which is available to authorized users.

✉ Mauro Papotti
mauro.papotti@unito.it

1 Department of Oncology, University of Turin, Turin, Italy

2 Department of Medical Sciences, University of Turin, Turin, Italy

3 Pathology Division, Candiolo Cancer Institute, FPO-IRCCS, Candiolo, Italy

4 Division of Orthopedics, Città della Salute e della Scienza di Torino Hospital, Turin, Italy

5 Division of Medical Oncology, Humanitas Gradenigo Hospital, Turin, Italy

6 Present Address: ASL Città di Torino, Turin, Italy

7 Candiolo Cancer Institute – FPO, IRCSS Candiolo, Turin, Italy

8 Anatomia Patologica, Città della Salute e della Scienza Hospital, University of Turin, Via Santena 7, 10126 Turin, Italy

Abbreviations

ABC	Aneurysmal bone cyst
DFI	Disease-free interval
FFPE	Formalin-fixed paraffin embedded
GC	Giant cell
GCTB	Giant cell tumor of bone
H&E	Hematoxylin and eosin
IHC	Immunohistochemistry
MTC	Mononuclear tumor cell
SD	Standard deviation
WHO	World Health Organization

Introduction

Giant cell tumors of bone (GCTB) are a well-defined clinicopathological and molecular entity, associated with a generally benign, but locally aggressive course, which represents approximately 5% of all primary bone tumors [1]. According to the last World Health Organization (WHO) classification, these tumors fall into the category of lesions

with intermediate behavior and locoregional aggressiveness, exceptionally developing distant metastases [2]. These tumors affect mature individuals, aged between 20 and 40, although occasionally may occur in children or in adults older than 65 years of age and typically arise in the epiphysis of long bones [2–4].

Morphologically, GCTB consists of a solid growth of mesenchymal mononuclear tumor cells (MTCs), roundish, of medium size, with bland atypia and a variable, occasionally high, number of mitotic figures, associated with a different amount of reactive multinucleated osteoclast-like giant cells (GCs). Nuclear factor NK-kβ ligand (RANKL) mediates osteoclast differentiation and activation by inducing a multinuclear osteoclast pattern, their migration and survival, eventually leading to the bone resorption phenomena that are commonly seen in GCTB [5–7]. Cell cycle fractions within the mononuclear cell compartment of GCTB can predict its progression-free survival, as recently demonstrated by Maros et al. [8], describing the elevated mitogenic potential and proliferative profile of these cells.

Driver mutations of GCTB have been identified in the *H3F3A* gene (a member of the Histone H3.3 family) [9, 10], with a G35W mutation present in approximately 96% of tested GCTB, thus supporting the notion that such an alteration is pathognomonic of these tumors. In order to routinely detect *H3F3A* alterations, a newly developed mutation-specific Histone 3.3 antibody proved highly reliable for the diagnosis of GCTB, with a sensitivity of approximately 95% [11, 12].

Current treatment options for GCTB include wide surgical resection, intralesional curettage or curettage with an adjuvant treatment [13]. While wide *en bloc* excision provides excellent local control, cases treated with curettage without adjuvant therapy may bear a higher risk of local recurrences [14–16].

A novel therapy using a RANKL inhibitor (Denosumab) to prevent bone resorption by giant osteoclast-like cells, thus favoring the subsequent surgical approach, has been introduced [17–19]. Since some literature data raised a concern of a possible higher rate of local recurrences in Denosumab-treated patients [20], its definitive role in GCTB management remains controversial [19, 21, 22]. Nonetheless, National Comprehensive Cancer Network (NCCN) guidelines clearly state that Denosumab treatment should be considered whenever upfront resection entails unacceptable morbidity and/or in case of inoperable axial lesions [23].

Currently, immunotherapy has become a standard of care for several human tumors, including melanoma and carcinomas [24, 25]. Moreover, immune checkpoint inhibitors are being increasingly investigated in various soft tissue and bone tumors with the aim of blocking the PD-1/PD-L1 axis activity [26–29].

Very recent data on 215 osteosarcomas [30] revealed their genomic and transcriptomic profiles of *PD-L1, PD-L2, B7-H3* and *IDO1*, suggesting the potential target for immunotherapeutic intervention. On the other hand, a study by Wang et al. [31] demonstrated that the combination of conventional chemotherapy and an anti-PD-L1 inhibitor might be effective in osteosarcoma.

Based on the above, the aim of the present study was: (i) to assess the expression of PD-L1 and Ki67 in a series of GCTB; (ii) to analyze the immune-related gene expression profile of these tumors by NanoString technology using a nCounter PanCancer Immune Profiling Panel compared to that of aneurysmal bone cysts (ABC); (iii) to correlate the results of the above-mentioned analyses with clinicopathological characteristics and outcomes.

Materials and methods

Case selection

All cases diagnosed as GCTB were retrieved from the pathology files of the Città della Salute e della Scienza Hospital of Torino in years 2004–2017: 50 cases were collected with available histological material and follow-up data. Radiological images and the hematoxylin and eosin (H&E) slides from each case were reviewed by three of us (JM, AL and MP). The diagnosis was eventually confirmed by morphology and immunohistochemistry (IHC) for mutant Histone 3.3 protein (see below) in 46 cases, which formed the basis of the present study. The remaining four cases were reclassified as other conditions upon revision and excluded. A control group of 24 cases of aneurysmal bone cyst (ABC), another benign giant cell-rich lesion, was retrieved from the same pathology file and time frame, after radiological and histomorphological verification of the diagnosis.

Clinicopathological data such as age at diagnosis, sex, tumor location, largest diameter of the lesion, type of treatment, Campanacci grade, pathologic fracture at presentation and follow-up data were collected from patients' clinical reports in a dedicated database. Before the study started, all cases were de-identified and coded by a pathology staff member not involved in the study, and all data were accessed anonymously.

Immunohistochemistry

Three-µm-thick sections were cut from a representative formalin-fixed paraffin-embedded (FFPE) tissue block of each case and stained with H&E or submitted to IHC. The latter was performed by an automated platform (Ventana BenchMark AutoStainer, Ventana Medical Systems, Tucson, AZ, USA) with the following primary antibodies: Histone

3.3 G35W mutation-specific rabbit monoclonal antibody (RM263, diluted 1:600, RevMAb Biosciences, San Francisco, USA); PD-L1 mouse monoclonal antibody (22C3, diluted 1:50, Dako Agilent, Santa Clara, USA); FOXP3 mouse monoclonal antibody (236A/E7, diluted 1:100, eBioscience, San Diego, USA). Antigen retrieval was performed using CC1 antigen retrieval buffer (pH 8.5, EDTA, 100 °C, 30 min; Ventana Medical Systems, AZ, USA) for all sections. Ultraview detection system was used throughout. Appropriate positive and negative controls were included for each immunohistochemical run.

In particular, the Histone 3.3 G35W mutation-specific antibody was evaluated as previously described, namely as having either negative or positive nuclear expression after incubation for 32 min at 36 °C [32].

PD-L1 was double dichotomized into (i) negative in case of $< 1\%$ cell expression or positive when immunoreactivity was observed in $\geq 1\%$ cells (ii) and expression by MTCs and GCs. Furthermore, PD-L1 interpretation in controversial cases was facilitated by double H3F3A/PD-L1 immunostainings, where the red H3F3A nuclear coloration better highlighted the tumor cells, having a continuous or discontinuous cell membrane PD-L1 expression, even in cases with weak reactivity. Histone 3.3 G35W and PD-L1 were assessed by visual estimation of the extent of immunoreactivity. FOXP3 was assessed counting the absolute number of tumor infiltrating lymphocytes in the whole tumor section and then dichotomized into two categories: 0–10 and ≥ 11 positive cells.

Gene expression analysis by NanoString technology

Gene expression analysis was performed on 48 samples having available tissue after IHC assessment. These included 38 GCTB and 10 ABC, as a control group. Eight GCTB samples were obtained from four patients, before and after treatment with Denosumab, in order to investigate the potential changes in the gene profile after systemic therapy.

For each sample, two 10-µm-thick FFPE tissue sections were obtained and collected in sterile Eppendorf tube. (The number of sections was increased in case of scant material.)

RNA isolation was performed using the FFPET RNA Isolation Kit (Roche Diagnostics GmbH, Mannheim, Germany), according to the manufacturer's protocols. Total RNA concentration was assessed using a NanoDrop spectrophotometer (Thermo Fisher Scientific, Inc., Wilmington, DE, USA). NanoString nCounter technology was used to measure relative expression levels of immune genes within the tumor microenvironment: 300 ng of total RNA from each sample was hybridized to the nCounter PanCancer Immune Profiling Panel, according to the manufacturer's instructions (NanoString Technologies, Seattle, WA, USA). This panel detects the expression of 770 mRNA targets: 730 immune-related genes and 40 housekeeping genes. The analyses were set up according to the protocol provided by the manufacturer. Expression data were normalized and analyzed with the nSolver analysis software (version 4.0.62). Samples obtained from the same patients were included only in additional analyses related to pre- and post-Denosumab treatment immunoprofiling. For background correction, the mean count of negative controls plus two times the standard deviation was subtracted from the counts for each gene. The means of the supplied positive controls and the geometric mean of the housekeeping genes were used to normalize the measured expression values. Both positive and negative controls were included in the panel, according to manufacturer's instructions. Additionally, the advanced analysis module (version 2.0.115) was used to perform differential expression analyses. Briefly, for each gene a single linear regression was fit using all selected covariates to predict expression. A volcano plot was generated to display each gene's -log10 (p value) and log2-fold change with the selected covariate. Highly statistically significant genes fell at the top of the plot above the horizontal lines, and highly differentially expressed genes fell to either side. Horizontal lines indicated various p value thresholds.

Normalized gene expression levels were obtained from nSolver, and analysis of RANK and RANKL differential expression between PD-L1-positive and PD-L1-negative cases was performed in GraphPad Prism software version 8.4.0 (GraphPad Software, Inc., San Diego, CA) using the t test (critical p value $= 0.05$).

Statistical analyses

All analyses were performed using Stata/MP 15.0 statistical software (STATA, College Station, TX). Continuous variables were summarized as the mean and standard deviation (SD), whereas for categorical variables, the frequency was provided. The patient's characteristics were compared using the Chi-square test for categorical variables and the t test or ANOVA test for continuous variables, according to Bonferroni corrections. Disease-free interval (DFI) was calculated from the date of primary lesion diagnosis to the date of recurrence or last follow-up. Survival curves between different groups were plotted using the Kaplan–Meier method, and the statistical comparisons were performed with log-rank test. Cox regression analyses were carried out on DFI to calculate HRs and 95% CIs for the different study groups. The proportional hazard assumption was assessed with the Schoenfeld residuals. This did not give reasons to suspect violation of this assumption.

Results

1. Clinicopathological characteristics and immunohistochemical profile

The clinical and pathological features of 46 GCTB cases are summarized in Table 1. Briefly, the median follow-up was 4.9 years, while median age at diagnosis was 34 years. The preferred location was the lower extremities (39/46) with tumors having a mean size of 6.4 cm. Majority of cases were treated with curettage (26/46). Locoregional recurrent disease occurred in 13 cases of GCTB. Most of the tumors were classified as Campanacci grade II (32/46). Denosumab treatment was administered to nine GCTB patients, only (six cases at diagnosis and three cases after the first recurrence). The GCTB group showed significantly larger lesions and higher number of fractures at presentation compared to ABC group.

2. Immunohistochemical profile

All GCTB had immunohistochemical positivity for the G35W mutation-specific Histone 3.3 antibody, with the majority of cases showing strong staining in the nuclei of the mononuclear cell population (Fig. 1a). No staining for the Histone 3.3 G35W mutation-specific antibody was observed in control cases of ABC.

PD-L1 positivity was observed in 13 of 46 (28.3%) GCTB and in only one of 24 (4.2%) ABC cases ($p = 0.016$) (Table 1). Positive cases had between PD-L1 reactivity

Table 1 Clinicopathological characteristics of a series of bone tumors with giant cells

		GCTB (46)	ABC (24)	Total (70)	p**
Median follow-up	Median (years) (25th–75th)	4.91 (2.36-5.58)	5.75 (3.48-6.63)	4.99 (3.41-6.28)	0.289
Age at diagnosis	Median (interval)	34 (17-77)	32 (15-70)	34 (17-77)	0.450
Gender	F	21	12	33	0.734
	M	25	12	37	
Site	Upper extremities	7	8	15	0.082
	Lower extremities	39	16	55	
Diameter lesion (cm)	≤ 5	17	18	35	0.002
	> 5	29	6	35	
Mean size (cm)	mean ± SD	6.42 ± 2.63	4.37 ± 1.67	5.72 ± 2.53	0.001
Surgical treatment	Curettage	26	12	38	0.732
	Resection	20	11*	31	
Recurrence	No	33	21	54	0.136
	Yes	13	3	16	
Campanacci grade	I	2	–	–	–
	II	32			
	III	12			
Fracture at presentation	No	41	23	64	0.342
	Yes	5	1	6	
Denosumab treatment	No	37	23	60	0.083
	Yes	9	1	10	
FOXP3	0–10 positive cells	26	19	45	0.061
	≥ 11 positive cells	20	5	25	
PD-L1	Negative	33	23	56	0.016
	Positive	13	1	14	
PD-L1	Negative	33	23	56	0.187
	Positive MTCs	5	0	5	
	Positive GCs	8	1	9	
Ki67	< 1%	8	13	21	0.001
	> 1%	38	11	49	
Ki67%	Mean ± SD	8.76 ± 9.97	3.54 ± 5.38	6.97 ± 8.99	0.020

*After initial biopsy, one case treated with transarterial embolization (TAE)

**Bonferroni correction

GCTB: giant cell tumor of bone, *ABC:* aneurysmal bone cyst

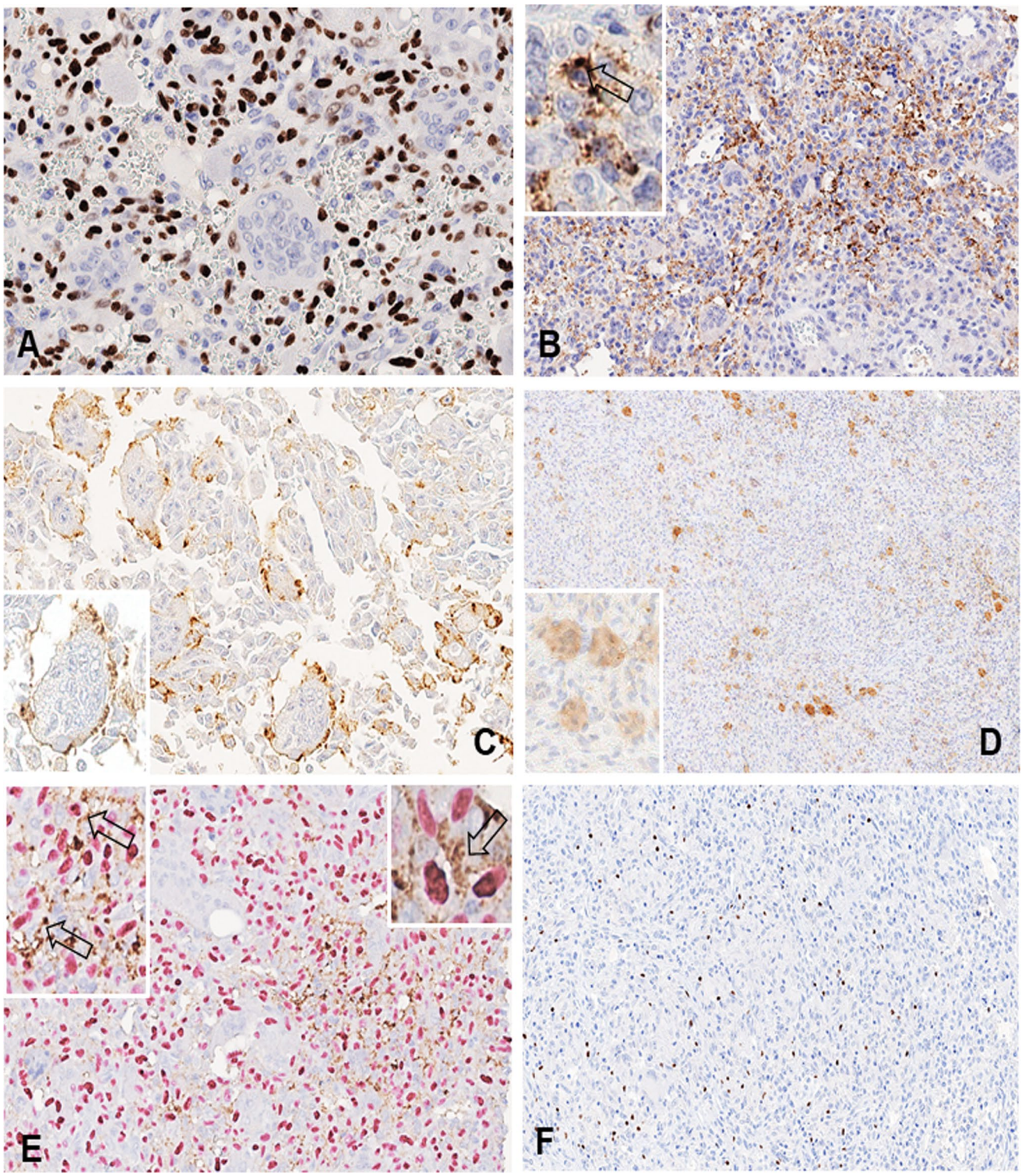

Fig. 1 **a** In a giant cell tumor of bone, strong immunoreactivity of neoplastic mononuclear stromal cells for H3.3 G35W mutation-specific antibody is present (400x). **b*** Strong PD-L1 immunoreactivity at the cell membrane of mononuclear stromal cells (200x, insert 400x). **c**, **d** PD-L1 expression by giant cells is mainly confined at the membrane level of the same giant cell (400x, insert 500x) and only occasionally occurs in the cytoplasm (80x, insert 200x). **e*** Double PD-L1 and H3F3A immunostaining in a controversial case of giant cell tumor of bone helps to distinguish neoplastic mononuclear stromal cells from adjacent immune cells (200x, inserts 400x and 500x). **f** FOXP3-positive tumor infiltrating lymphocytes in a case of giant cell tumor of bone (200x). *The arrows in images B and E indicate mononuclear tumor cells reactive for PD-L1

ranging from 1 to 20%, except for one case that displayed 30% of cell immunoexpression. In five cases, the reactivity was observed in MTCs (Fig. 1b) and in eight cases in reactive GCs with either membranous or cytoplasmic pattern (Fig. 1c, d). The distinction of neoplastic mononuclear cells from adjacent immune cells (macrophages and lymphocytes) was based on morphology and supported by a double PD-L1 and H3F3A immunostaining in controversial cases (Fig. 1e).

Additionally, PD-L1 was also tested in four Denosumab-treated patients in which both samples (before and after treatment) were available: One case was negative in both specimens, and three were positive before treatment. Of these latter, only one preserved PD-L1 expression in the specimen resected after treatment and the remaining two completely lost their PD-L1 reactivity.

Moreover, no significant difference was observed between GCTB subset and the group of ABCs in FOXP3-positive tumor infiltrating lymphocytes ($p = 0.061$, Table 1).

Furthermore, we stratified our series by PD-L1 expression (Table 2), and the correlation with recurrent disease remained significant ($p = 0.006$), as well as its correlation with higher Ki67 proliferation index ($p = 0.024$). In addition, in 9/14 (64%) PD-L1-positive cases more abundant FOXP3-positive tumor infiltrate was observed (> 11 positive cells) compared to PD-L1-negative samples (16/56, 28%) ($p = 0.013$).

3. PD-L1 expression and its impact on prognosis

By univariate analysis (Table 3), Campanacci classification, surgical resection and PD-L1 expression were significantly related to DFI. In particular, PD-L1 expression was associated with a poorer DFI (HR = 4.15, CI 1.52-11.31; $p = 0.005$). When stratified according to the positive cell population (MTCs *versus* GCs), the expression of this marker maintained a significant HR for both cellular types, being higher in PD-L1-positive MTCs than multinucleated GCs (HR = 6.11 *versus* HR = 3.34, respectively).

Kaplan–Meier survival analysis also confirmed these results (Fig. 2a, b): DFI was significantly longer in PD-L1-negative *versus* PD-L1-positive cases (log-rank test $p = 0.0026$), while among PD-L1-positive cases, the worst outcome was seen in cases with expression by MTC (rather than multinucleated GCs) (log-rank test $p = 0.0045$).

Table 2 Case series stratified by PD-L1 expression

		PD-L1 negative (56)	PD-L1 positive (14)	Total (70)	*p***
Age at diagnosis	Median (interval)	34 (17-77)	35(21-71)	34 (17-77)	0.664
Gender	F	28	5	33	0.345
	M	28	9	37	
Site	Upper extremities	14	1	15	0.149
	Lower extremities	42	13	55	
Diameter lesion (cm)	≤ 5	31	4	35	0.075
	> 5	25	10	35	
Mean size (cm)	mean ± SD	5.51 ± 2.57	6.52 ± 2.28	5.72 ± 2.53	0.187
Surgical treatment*	Curettage	28	10	38	0.168
	Resection	27	4	31	
Fracture at presentation	No	52	12	64	0.393
	Yes	4	2	6	
Campanacci	I	2	0	2	0.625
	II	23	9	32	
	III	8	4	12	
Recurrence	No	47	7	54	0.006
	Yes	9	7	16	
Denosumab treatment	No	50	10	60	0.090
	Yes	6	4	10	
FOXP3	0–10 positive cells	40	5	45	0.013
	≥ 11 positive cells	16	9	25	
Ki67	< 1%	21	19	2	0.156
	> 1%	49	37	12	
Ki67%	Mean ± SD	6.97 ± 8.99	5.76 ± 8.27	11.78 ± 10.4	0.024

*After initial abundant biopsy, one ABC case was treated with transarterial embolization (TAE)

**Bonferroni correction

Table 3 Cox Regression analyses of DFI

DFI	HR	CI	p
Age (linear)	0.99	0.96–1.03	0.631
Gender (M vs. F)	1.67	0.61–4.61	0.318
Site (lower vs. upper extremities)	4.32	0.57–32.74	0.157
Diameter (> 5 cm)	1.65	0.60–4.54	0.333
Surgical treatment resection versus curettage	0.26	0.07–0.93	0.038
GCTB versus ABC	2.76	0.78–9.73	0.113
PD-L1 (negative vs positive)	4.15	1.52–11.31	0.005
PD-L1			
Negative	1		
Positive MTCs	6.11	1.63–22.9	0.007
Positive GCs	3.34	1.02–11.00	0.047
FOXP3			
> 11 positive cells	1.63	0.61–4.39	0.331
Ki67 (< 1% vs. ≥ 1%)	2.14	0.61–7.53	0.234
Campanacci*	4.28	1.48–12.36	0.007
Fracture (yes vs. no)	1.35	0.31–5.96	0.688

*Referred only to GCTB

GCTB: giant cell tumor of bone, *ABC:* aneurysmal bone cyst, *MTC:* mononuclear tumor cell, *GC:* giant cell

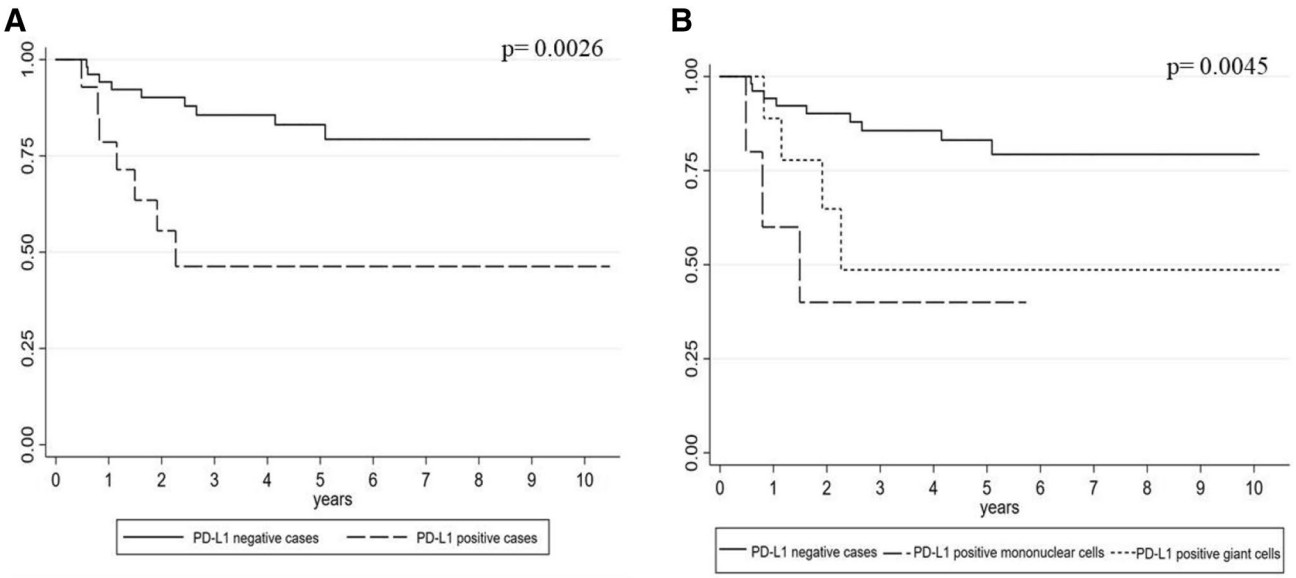

Fig. 2 **a** Kaplan–Meier curve of DFI according to PD-L1 expression in giant cell tumor of bone (log-rank test $p = 0.0026$). **b** Kaplan–Meier curve of DFI according to PD-L1 expression in different cell types of giant cell tumor of bone (log-rank test $p = 0.0045$)

4. Expression profile of immune-related genes by NanoString technology

(a) Gene expression profile according to PD-L1 levels

In order to identify which genes are possibly correlated with the expression of PD-L1 and the risk of recurrence, expression levels of immune response-related genes were compared between the groups of PD-L1-positive and PD-L1-negative cases.

Stratifying cases according to PD-L1 expression, *CD27*, *CD6*, *IL10* ($p < 0.01$), and *TIGIT*, *OSM*, *CFP, LILRA1, CD1D* ($p < 0.05$) genes showed significantly higher expression levels in PD-L1-positive cases (Fig. 3a, green rectangle). In addition, a reduced expression of *LCK* and *TLR8*

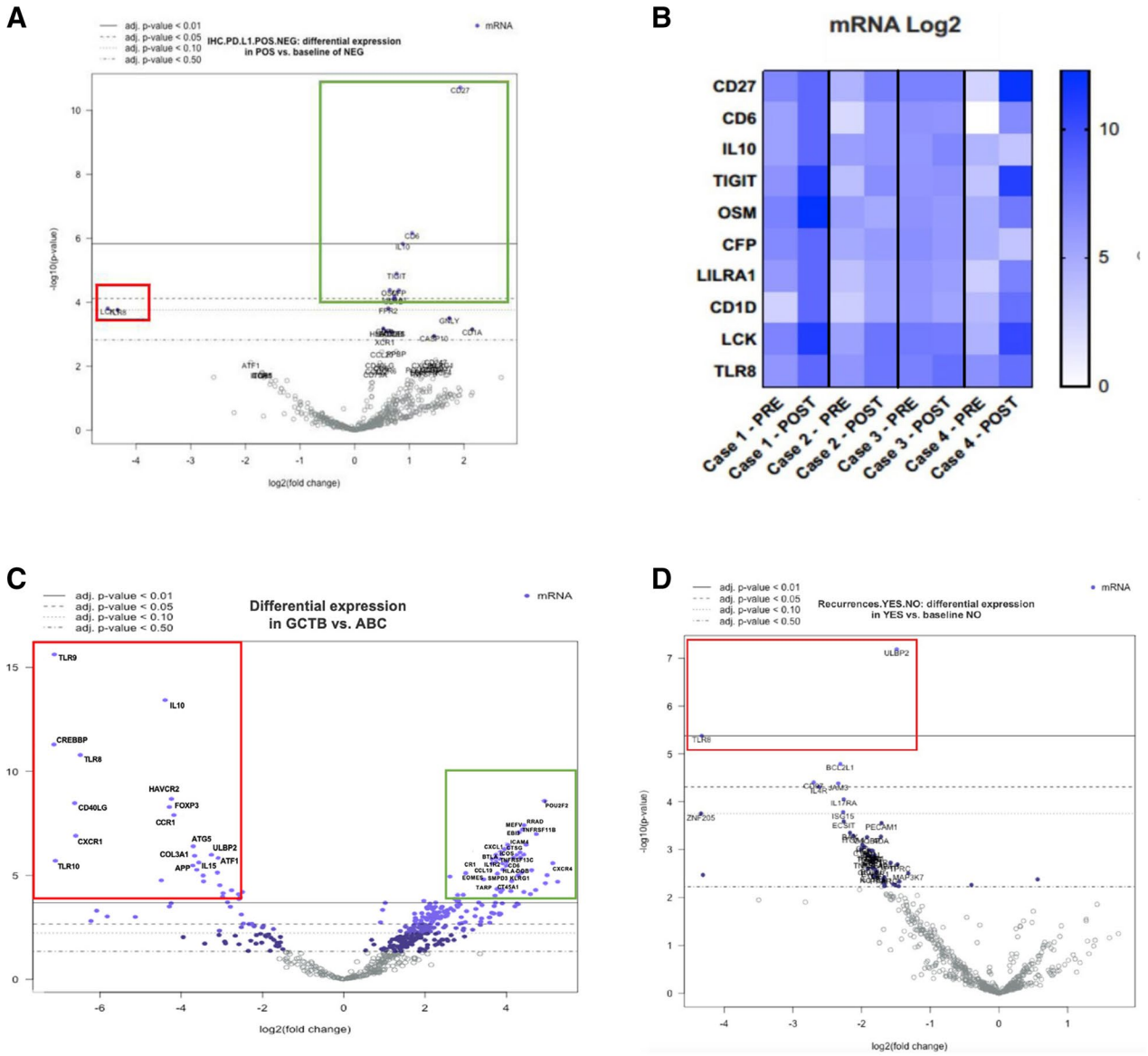

Fig. 3 **a** Different gene expression profiles according to PD-L1 immunoreactivity. Upregulated genes *CD27*, *CD6*, *IL10* ($p < 0.01$) are marked by the green rectangle. Red rectangle highlights downregulated genes *LCK* and *TLR8* although not reaching statistical significance ($p = 0.06$). **b** Different gene expressions in cases pre- and post-treatment with Denosumab. Particularly, cases 1 and 4 show higher levels of *CD27, CD6, TIGIT, OSM, LCK* and *TLR8* genes in the post-treatment samples compared to those of initial biopsies. **c** Giant cell tumors of bone, compared to aneurysmal bone cysts, show significantly higher expression of *MEFV*, *TNFRSF11B*, *EBI3*, *CXCL1, ICOS*, *CD6*, *CCL19*, *CR1*, *EOMES*, *KLRG1* and *CXCR4* genes ($p < 0.01$) indicated by the green rectangle. Downregulated genes *TLR9*, *IL10*, *TLR8*, *FOXP3*, *CXCR1*, *ATG5, ATF1* and *IL15* ($p < 0.01$) are marked by the red rectangle. **d** *TLR8* and *ULBP2* genes were found significantly downregulated in giant cell tumors of bone that developed locoregional recurrences

genes was detected, although not reaching statistical significance ($p = 0.06$) (Fig. 3a, red rectangle).

With the limitations of the small sample size, changes of single gene expression profiles were recorded in samples before and after Denosumab treatment. It can be noted that, case 1 and 4 had higher expression levels of *CD27, CD6, TIGIT, OSM, LCK* and *TLR8* genes in post-treatment samples compared to those of initial biopsies (Fig. 3b).

Moreover, single gene exploration analysis of *RANK* ($p = 0.43$) and *RANKL* ($p = 0.39$) in the group of GCTB according to PD-L1 levels did not demonstrate significant differences in the gene expression levels (Supplementary Fig. 1).

(b) Gene regulation in GCTB *versus* ABC

Furthermore, we observed up- and downregulation of immune response-related genes in GCTB. Compared to the control group of ABCs, a significantly higher expression ($p < 0.01$) was observed for *MEFV*, *TNFRSF11B*, *EBI3*, *CXCL1, ICOS*, *CD6*, *CCL19*, *CR1*, *EOMES*, *KLRG1* and *CXCR4* genes (Fig. 3c, green rectangle). On the other hand, downregulated genes included: *TLR9*, *IL10*, *TLR8*, *FOXP3*, *CXCR1*, *ATG5, ATF1* and *IL15* ($p < 0.01$) (Fig. 3c red rectangle).

In addition, the gene expression levels identified by the PanCancer Immune Profiling Panel highlighted a profile linked to the macrophage functions in GCTB (Supplementary Fig. 2).

5. Recurrent GCTB disease and gene expression characterization

Differences among GCTB cases that developed recurrent disease were also looked for, and a statistically significant reduced expression ($p < 0.01$) was observed in only two genes, namely *ULBP2* and *TLR8,* compared to nonrecurrent tumors (Fig. 3d).

Discussion

GCTB is a locally aggressive neoplasm, with a low percentage of patients developing lung metastases and having an adverse outcome. Recurrence is reported in approximately 15% to 50% of cases. A driver mutation in gene H3F3A (G35W) has been described, distinguishing unequivocally GCTB from other giant cell containing bone lesions, such as ABCs.

As expected [16, 33], this study confirms that Campanacci classification and surgery treatment are related to a different clinical outcome in our series of patients. More importantly, this is the first study that demonstrates a significant correlation between PD-L1 expression and local recurrence in GCTB, in association with a specific profile of immune system-related genes, as detected by NanoString technology.

So far, PD-L1 (and PD-1) overexpression has been correlated with adverse prognosis in other bone tumors as well as in soft tissue tumors [34–36].

In GCTB, PD-L1 expression is significantly related to higher risk of recurrence in terms of DFI, suggesting a more anergic immune status, which may favor escape mechanisms and recurrence development. This hypothesis is supported by an idiosyncratic gene expression signature detected by NanoString technology in PD-L1-positive tumors. In fact, these latter had three genes significantly upregulated, including *CD27, CD6* and *IL10. CD27* is reported to be expressed by osteoclast precursors, according to the "macrophage-like" or "osteoclast-like" pattern of GCs [37], and therefore, a higher expression of this marker in PD-L1-positive lesions may probably be related to a less differentiated phenotype of GCs. Likewise, the upregulation of *CD6* and *IL-10* may be associated with maturation of GCs. In fact, T regulatory cells (Treg) inhibit osteoclast maturation in bone tissue, producing IL4 and IL10. Furthermore, CD6 is a general attenuator of T cell activation [38, 39], in line with the hypothesis of a more anergic status of immune system in PD-L1-positive tumors and consequent higher risk of recurrence. Certainly, the microenvironment of GCTB is complex due to the presence of neoplastic cells that recruit mononuclear osteoclast precursors and promote their maturation in multinuclear osteoclasts [40]. However, it has been discovered that multinucleated GC per se is able to continuously produce rapidly proliferating mononucleated cells by a budding process [41]. In a more recent study [42], the authors described giant cell cycle, i.e., giant cancer cell self-renewal mechanism via endoreduplication and nuclear budding or fragmentation, producing small daughter nuclei. Consequently, these nuclei obtain cytoplasm, separate from the giant mother cells and acquire competency in mitosis. This dynamic self-proliferation of GC may explain their more immature phenotype, in contrast to the phenotype of dedifferentiated malignant lesions.

In addition, in such PD-L1-positive tumors, a couple of genes (*TLR8* and *LCK)* were found to be downregulated, even if the difference compared to PD-L1-negative tumors had borderline significance ($p = 0.06$), only. *TLR8* is a member of the Toll-like receptor (TLR) family which plays an essential role in pathogen recognition and activation of innate immunity [43]. *LCK* is a key signaling molecule in the selection and maturation of developing T cells that binds to surface receptors present in various cells including CD4 and CD8 lymphocytes. The relatively low number of the present series did not allow to achieve statistical significance across *TLR8* and *LCK* expression, but despite this, in analyzed samples pre- and post-treatment with Denosumab, we observed again a different modulation of these genes and, similarly, in recurrent lesions, *TLR8* showed a reduced expression. In line with our preliminary observations, several authors have described [44] that Denosumab-based RANKL targeting may reinforce natural killer (NK) cell-mediated antitumor responses and that NK-cell activation has been regulated directly by *TLR8* and *LCK* [45, 46]. Moreover, Francisconi and colleagues have studied immunoregulatory role of RANKL in a mouse model, suggesting its continuous interference with Treg activity [47].

These data support the hypothesis that *TLR8* and *LCK* downregulation might be associated with a less reactive environment in PD-L1-positive cases, related to an "escape" mechanism of GCTB, and open new scenarios in the treatment of these lesions.

In fact, despite the limitations of this study related to its retrospective nature, the relatively small sample size and the different surgical treatments, the current findings highlight that PD-L1 expression is related to a higher risk of recurrence with a "specific immunoprofiling pattern." Therefore, the possible use of immune checkpoint inhibitors of the PD-1/PD-L1 axis might be considered for the treatment of selected clinically aggressive GCTB cases after resection, including those with disease relapse or metastatic localizations or those in which surgical treatment might be challenging due to disease location within complex anatomical structures (in particular, axial skeleton). Although Denosumab proved useful to prevent bone resorption by giant osteoclast-like cells, several controversies concerning optimal treatment dose, duration and interval and drug safety still remain [48]. The option of immunotherapy in GCTB could find support in a recent work by Ayers and co-workers [49], who identified an 18-gene T cell-inflamed signature (named Tumor Inflammation Signature, TIS), able to predict response to Pembrolizumab across multiple solid tumors. Two of the genes identified as significantly upregulated in PD-L1-positive GCTB (*CD27* and *TIGIT*) in the present series are also included in the Ayers' proposed signature and are overexpressed in responder patients. Moreover, the applicability of the TIS algorithm to gene expression data from The Cancer Genome Atlas (TCGA) database across different histologically defined tumor types was also demonstrated [50]. Finally, elevated levels of *CD27* were also observed in a recent study by Klein and co-workers [51] in a series of dermal sarcomas, confirming the potential role of the currently identified upregulated gene panel also in other human tumors.

To the best of our knowledge, this is the first study that reports GCTB gene expression profile detected by NanoString technology and demonstrates association of PD-L1 immunoexpression to a higher risk of recurrence, possibly mediated by the inhibition of the host immune system and the development of an anergic environment, as indicated by the significant upregulation of genes involved in immune response modulation. Our findings encourage PD-L1 immunohistochemical evaluation at diagnosis to select GCTB patients at higher risk of recurrence, who may potentially be considered for anti-PD-1/PD-L1 therapies.

Acknowledgments We would like to thank Mr. Lorenzo Visca for his skillful technical assistance. This study is dedicated to the memory of Tom, an extraordinarily lively boy who untimely died of cancer.

Authors' contribution MP designed and supervised the study. JM and AL collected the data and prepared the material. LA, JM, CM, FV and CV analyzed the samples. AC, GG, RP and NR treated and followed patients and provided clinical data. SOA performed statistical analyses. MP, JM, LA, SOA, AL, LB and PC contributed to data interpretation. The first draft of the manuscript was written by MP and JM, and all authors critically revised the manuscript. All authors read and approved the final version of the manuscript.

Funding This work was partially supported by an unrestricted grant (1704/2018) from the "Fondazione per i Tumori muscolo scheletrici," Torino. In addition, this research received funding specifically dedicated to the Department of Medical Sciences from Italian Ministry for Education, University and Research (Ministero dell'Istruzione, dell'Università e della Ricerca—MIUR) under the program "Dipartimenti di Eccellenza 2018–2022," Project no D15D18000410001. JM and LB are PhD fellows at the University of Turin. LA is funded by Fondazione Umberto Veronesi (Postdoctoral fellowship 2018 and 2019).

Compliance with Ethical Standards

Conflict of Interest The authors declare that they have no conflict of interest.

Ethical approval and ethical standards This study was conducted in accordance with the ethical standards of the Declaration of Helsinki, and approval was granted by the Research Ethics Committee for Human Biospecimen Utilization (Department of Medical Sciences—ChBU) of the University of Turin (n° 10/2019). This study does not contain any studies with human participants or animals performed by any of the authors.

Informed consent Before the study started, all cases were de-identified and coded by a pathology staff member not involved in the study, and all data were accessed anonymously. Considering the retrospective nature of this research protocol with no impact on patients' treatment and the use of anonymized data only, no written consent was required by the Committee.

REFERENCES

1. Cowan RW, Singh G (2013) Giant cell tumor of bone: a basic science perspective. Bone 52:238–246. https://doi.org/10.1016/j.bone.2012.10.002
2. Athanasou NA, Bansal M, Forsyth R, Reid RP, Sapi Z (2013) Giant cell tumour of bone. In: Fletcher CDM, Bridge JA, Hogendoorn PCW, Mertens F (eds) WHO classification of tumours of soft tissue and bone, 4th edn. IARC Press, Lyon, pp 321–324
3. Errani C, Ruggieri P, Asenzio MA, Toscano A, Colangeli S, Rimondi E et al (2010) Giant cell tumor of the extremity: a review of 349 cases from a single institution. Cancer Treat Rev 36:1–7. https://doi.org/10.1016/j.ctrv.2009.09.002
4. Werner M (2006) Giant cell tumour of bone: morphological, biological and histogenetical aspects. Int Orthop 30:484–489. https://doi.org/10.1007/s00264-006-0215-7
5. Luo G, Li F, Li X, Wang ZG, Zhang B (2018) TNF-α and RANKL promote osteoclastogenesis by upregulating RANK via the NF-κB pathway. Mol Med Rep 17:6605–6611. https://doi.org/10.3892/mmr.2018.8698
6. Atkins GJ, Haynes DR, Graves SE, Evdokiou A, Hay S, Bouralexis S, Findlay DM (2000) Expression of osteoclast differentiation signals by stromal elements of giant cell tumors. J Bone Miner Res 15:640–649. https://doi.org/10.1359/jbmr.2000.15.4.640

7. Boyle WJ, Simonet WS, Lacey DL (2003) Osteoclast differentiation and activation. Nature 423:337–342. https://doi.org/10.1038/nature01658
8. Maros ME, Schnaidt S, Balla P, Kelemen Z, Sapi Z et al (2019) In situ cell cycle analysis in giant cell tumor of bone reveals patients with elevated risk of reduced progression-free survival. Bone 127:188–198. https://doi.org/10.1016/j.bone.2019.06.022
9. Kervarrec T, Collin C, Larousserie F, Bouvier C, Aubert S, Gomez-Brouchet A et al (2017) H3F3 mutation status of giant cell tumors of the bone, chondroblastomas and their mimics: a combined high resolution melting and pyrosequencing approach. Mod Pathol 30:393–406. https://doi.org/10.1038/modpathol.2016.212
10. Righi A, Mancini I, Gambarotti M, Picci P, Gamberi G, Marraccini C et al (2017) Histone 3.3 mutations in giant cell tumor and giant cell-rich sarcomas of bone. Hum Pathol 68:128–135. https://doi.org/10.1016/j.humpath.2017.08.033
11. Lüke J, von Baer A, Schreiber J, Lübbehüsen C, Breining T, Mellert K et al (2017) H3F3A mutation in giant cell tumour of the bone is detected by immunohistochemistry using a monoclonal antibody against the G34W mutated site of the histone H3.3 variant. Histopathology 71:125–133. https://doi.org/10.1111/his.13190
12. Presneau N, Baumhoer D, Behjati S, Pillay N, Tarpey P, Campbell PJ et al (2015) Diagnostic value of H3F3A mutations in giant cell tumour of bone compared to osteoclast-rich mimics. J Pathol Clin Res 1:113–123. https://doi.org/10.1002/cjp2.13
13. Montgomery C, Couch C, Emory CL, Nicholas R (2019) Giant cell tumor of bone: review of current literature, evaluation, and treatment options. J Knee Surg 32:331–336. https://doi.org/10.1055/s-0038-1675815
14. Chen L, Ding XY, Wang CS, Si MJ, Du LJ, Zhang WB, Lu Y (2014) In-depth analysis of local recurrence of giant cell tumour of bone with soft tissue extension after intralesional curettage. Radiol Med 119:861–870. https://doi.org/10.1007/s11547-014-0396-x
15. Errani C, Tsukamoto S, Leone G, Akahane M, Cevolani L, Tanzi P et al (2017) Higher local recurrence rates after intralesional surgery for giant cell tumor of the proximal femur compared to other sites. Eur J Orthop Surg Traumatol 27:813–819. https://doi.org/10.2106/JBJS.17.00057
16. Lausten GS, Jensen PK, Schiødt T, Lund B (1996) Local recurrences in giant cell tumour of bone. Long-term follow up of 31 cases. Int Orthop 20:172–176. https://doi.org/10.1007/s002640050057
17. Branstetter DG, Nelson SD, Manivel JC, Blay JY, Chawla S, Thomas DM et al (2012) Denosumab induces tumor reduction and bone formation in patients with giant-cell tumor of bone. Clin Cancer Res 18:4415–4424. https://doi.org/10.1158/1078-0432.CCR-12-0578
18. Luengo-Alonso G, Mellado-Romero M, Shemesh S, Ramos-Pascua L, Pretell-Mazzini J (2019) Denosumab treatment for giant-cell tumor of bone: a systematic review of the literature. Arch Orthop Trauma Surg. https://doi.org/10.1007/s00402-019-03167-x
19. Chawla S, Henshaw R, Seeger L, Choy E, Blay JY, Ferrari S et al (2013) Safety and efficacy of denosumab for adults and skeletally mature adolescents with giant cell tumour of bone: interim analysis of an open-label, parallel-group, phase 2 study. Lancet Oncol 14:901–908. https://doi.org/10.1016/S1470-2045(13)70277-8
20. Errani C, Tsukamoto S, Leone G, Righi A, Akahane M, Tanaka Y, Donati DM (2018) Denosumab may increase the risk of local recurrence in patients with giant-cell tumor of bone treated with curettage. J Bone Joint Surg Am 100:496–504. https://doi.org/10.2106/JBJS.17.00057
21. van der Heijden L, Dijkstra PDS, Blay JY, Gelderblom H (2017) Giant cell tumour of bone in the denosumab era. Eur J Cancer 77:75–83. https://doi.org/10.1016/j.ejca.2017.02.021
22. Errani C, Tsukamoto S, Mavrogenis AF (2017) How safe and effective is denosumab for bone giant cell tumour? Int Orthop 41:2397–2400. https://doi.org/10.1007/s00264-017-3536-9
23. NCCN Clinical Practice Guidelines in Oncology (NCCN Guidelines®). Bone Cancer. https://www.nccn.org/professionals/physician_gls/default.aspx#site Accessed 26 June 2019
24. Domingues B, Lopes JM, Soares P, Pópulo H (2018) Melanoma treatment in review. Immunotargets Ther 7:35–49. https://doi.org/10.2147/ITT.S134842
25. Yu Y, Cui J (2018) Present and future of cancer immunotherapy: a tumor microenvironmental perspective. Oncol Lett 16:4105–4113. https://doi.org/10.3892/ol.2018.9219
26. Wang Z, Wang Z, Li B, Wang S, Chen T, Ye Z (2019) Innate immune cells: a potential and promising cell population for treating osteosarcoma. Front Immunol 10:1114. https://doi.org/10.3389/fimmu.2019.01114
27. Uehara T, Fujiwara T, Takeda K, Kunisada T, Ozaki T, Udono H (2015) Immunotherapy for bone and soft tissue sarcomas. Biomed Res Int 2015:820813. https://doi.org/10.1155/2015/820813
28. Zheng W, Xiao H, Liu H, Zhou Y (2015) Expression of programmed death 1 is correlated with progression of osteosarcoma. APMIS 123:102–107. https://doi.org/10.1111/apm.12311
29. Torabi A, Amaya CN, Wians FH Jr, Bryan BA (2017) PD-1 and PD-L1 expression in bone and soft tissue sarcomas. Pathology 49:506–513. https://doi.org/10.1016/j.pathol.2017.05.003
30. McEachron TA, Triche TJ, Sorenson L, Parham DM, Carpten JD (2018) Profiling targetable immune checkpoints in osteosarcoma. Oncoimmunology 7:e1475873. https://doi.org/10.1080/2162402X.2018.1475873
31. Wang J, Hu C, Wang J, Shen Y, Bao Q, He F et al (2019) Checkpoint blockade in combination with doxorubicin augments tumor cell apoptosis in osteosarcoma. J Immunother. https://doi.org/10.1097/CJI.0000000000000281
32. Rehkämper J, Steinestel K, Jeiler B, Elges S, Hekeler E, Huss S et al (2018) Diagnostic tools in the differential diagnosis of giant cell-rich lesions of bone at biopsy. Oncotarget 9:30106–30114. https://doi.org/10.18632/oncotarget.25725
33. Urakawa H, Yonemoto T, Matsumoto S, Takagi T, Asanuma K, Watanuki M et al (2018) Clinical outcome of primary giant cell tumor of bone after curettage with or without perioperative denosumab in Japan: from a questionnaire for JCOG 1610 study. World J Surg Oncol 16:160. https://doi.org/10.1186/s12957-018-1459-6
34. Yoshida K, Okamoto M, Sasaki J, Kuroda C, Ishida H, Ueda K et al (2019) Clinical outcome of osteosarcoma and its correlation with programmed death-ligand 1 and T cell activation markers. Onco Targets Ther 12:2513–2518. https://doi.org/10.2147/OTT.S198421
35. Kim JR, Moon YJ, Kwon KS, Bae JS, Wagle S, Kim KM et al (2013) Tumor infiltrating PD1-positive lymphocytes and the expression of PD-L1 predict poor prognosis of soft tissue sarcomas. PLoS One 8:e82870. https://doi.org/10.1371/journal.pone.0082870
36. Kim C, Kim EK, Jung H, Chon HJ, Han JW, Shin KH et al (2016) Prognostic implications of PD-L1 expression in patients with soft tissue sarcoma. BMC Cancer 16:434. https://doi.org/10.1186/s12885-016-2451-6
37. Xiao Y, Song JY, de Vries TJ, Fatmawati C, Parreira DB, Langenbach GE et al (2013) Osteoclast precursors in murine bone marrow express CD27 and are impeded in osteoclast development by CD70 on activated immune cells. Proc Natl Acad Sci USA 110:12385–12390. https://doi.org/10.1073/pnas.1216082110

38. Bozec A, Zaiss MM (2017) T regulatory cells in bone remodelling. Curr Osteoporos Rep 15:121–125. https://doi.org/10.1007/s11914-017-0356-1
39. Oliveira MI, Gonçalves CM, Pinto M, Fabre S, Santos AM, Lee SF et al (2012) CD6 attenuates early and late signaling events, setting thresholds for T-cell activation. Eur J Immunol 42:195–205. https://doi.org/10.1002/eji.201040528
40. Kato I, Furuya M, Matsuo K, Kawabata Y, Tanaka R, Ohashi K (2018) Giant cell tumours of bone treated with denosumab: histological, immunohistochemical and H3F3A mutation analyses. Histopathology 72:914–922. https://doi.org/10.1111/his.13448
41. Solari F, Domenget C, Gire V, Woods C, Lazarides E, Rousset B, Jurdic P (1995) Multinucleated cells can continuously generate mononucleated cells in the absence of mitosis: a study of cells of the avian osteoclast lineage. J Cell Sci 108:3233–3241
42. Niu N, Zhang J, Zhang N, Mercado-Uribe I, Tao F, Han Z et al (2016) Linking genomic reorganization to tumor initiation via the giant cell cycle. Oncogenesis 5:e281. https://doi.org/10.1038/oncsis.2016.75
43. Janssens S, Beyaert R (2003) Role of Toll-like receptors in pathogen recognition. Clin Microbiol Rev 16:637–646. https://doi.org/10.1128/CMR.16.4.637-646.2003
44. Schmiedel BJ, Grosse-Hovest L, Salih HR (2013) A "vicious cycle" of NK-cell immune evasion in acute myeloid leukemia mediated by RANKL? Oncoimmunology 2:e23850. https://doi.org/10.4161/onci.23850
45. Gorski KS, Waller EL, Bjornton-Severson J, Hanten JA, Riter CL, Kieper WC et al (2006) Distinct indirect pathways govern human NK-cell activation by TLR-7 and TLR-8 agonists. Int Immunol 18:1115–1126. https://doi.org/10.1093/intimm/dxl046
46. Huang L, Zhu P, Xia P, Fan Z (2016) WASH has a critical role in NK cell cytotoxicity through Lck-mediated phosphorylation. Cell Death Dis 7:e2301. https://doi.org/10.1038/cddis.2016.212
47. Francisconi CF, Vieira AE, Azevedo MCS, Tabanez AP, Fonseca AC, Trombone APF et al (2018) RANKL triggers treg-mediated immunoregulation in inflammatory osteolysis. J Dent Res 97:917–927. https://doi.org/10.1177/0022034518759302
48. Palmerini E, Chawla NS, Ferrari S, Sudan M, Picci P, Marchesi E et al (2017) Denosumab in advanced/unresectable giant-cell tumour of bone (GCTB): for how long? Eur J Cancer 76:118–124. https://doi.org/10.1016/j.ejca.2017.01.028
49. Ayers M, Lunceford J, Nebozhyn M, Murphy E, Loboda A, Kaufman DR et al (2017) IFN-γ-related mRNA profile predicts clinical response to PD-1 blockade. J Clin Invest 127:2930–2940. https://doi.org/10.1172/JCI91190
50. Danaher P, Warren S, Lu R, Samayoa J, Sullivan A, Pekker I et al (2018) Pan-cancer adaptive immune resistance as defined by the Tumor Inflammation Signature (TIS): results from The Cancer Genome Atlas (TCGA). J Immunother Cancer 6:63. https://doi.org/10.1186/s40425-018-0367-1
51. Klein S, Mauch C, Wagener-Ryczek S, Schoemmel M, Buettner R, Quaas A et al (2019) Immune-phenotyping of pleomorphic dermal sarcomas suggests this entity as a potential candidate for immunotherapy. Cancer Immunol Immunother 68:973–982. https://doi.org/10.1007/s00262-019-02339-3